Brackish water desalination using electrodialysis: predictive mass transfer and concentration distribution model along the electrodialyzer

Azadeh Ghorbani and Abbas Ghassemi

ABSTRACT

This study employs theory and experimental data from a laboratory-scale electrodialyzer to predict sodium chloride (NaCl) mass transport and concentration distribution along the electrodialyzer as a function of feed concentration, feed flow rate, applied voltage, and pressure. Moreover, a model was developed to predict the ion removal as a function of driving forces through solving the complete Navier–Stokes, continuity, and steady state Nernst–Planck equations by the finite difference numerical method. The findings of the experiments confirmed that concentration distributions are nonlinear along both the dilute and concentrate compartments. The results also demonstrated that increases in pressure and feed flow rate have a negative effect on salt removal, linear and nonlinear for pressure and flow rate, respectively. In the investigated ranges, higher voltage increased salt removal at a constant feed concentration.

Key words | concentration distribution, desalination, laboratory scale electrodialysis, predictive model

Azadeh Ghorbani (corresponding author)
Abbas Ghassemi
Department of Chemical and Materials Engineering,
New Mexico State University,
Las Cruces, NM 88003,
USA
E-mail: *azadeh12@nmsu.edu*

LIST OF SYMBOLS

c Salt concentration (mole·m^{-3})
D Ion-diffusion coefficient (m^2·s^{-1})
e Electron charge (c)
E Electric field (v)
F Faraday constant
i Current density (A·m^{-2})
H Thickness of the channel (m)
L Channel length (m)
k_b Boltzmann constant (J·K^{-1})
n_0 Ion density (mole·m^{-3})
p Pressure component
R Universal gas constant (J·mole^{-1}·K^{-1})
T Solution temperature (K)
u Velocity component (m·s^{-1})
z Ionic charge

GREEK LETTERS

φ Electric potential (v)
α Ionic energy parameter
ε Dielectric constant
ζ Zeta potential (v)
ω Debye–Huckel parameter (m^{-1})

INTRODUCTION

Electrodialysis (ED) is a membrane-based desalination technology in which ions are transferred through ion-exchange membrane under the influence of an applied electrical field. ED systems have been applied for over 50 years in the desalination of brackish water and are among the most important desalination methods (Valerdi-Perez *et al.* 2001; Kabay *et al.* 2003; Strathmann 2010; Zhang *et al.* 2011). The mass transport in ED – movement of ions through the ion-exchange membrane – plays the primary role in determining the overall performance of system. Therefore, increased understanding of mass transport in ED systems provides the knowledge for optimizing their performance.

doi: 10.2166/wst.2017.547

The mass transport phenomenon determines the desalination rate and the quality of the desalinated water, so multiple theoretical and experimental studies have been conducted to describe and predict mass transport. From a theoretical perspective, the mass transport phenomena in ED can be described through the Nernst–Planck equation (Mitko & Turek 2014). The total flux of ions in the ED process (the mass transport) is driven by three components – diffusion driven by the concentration gradient, migration driven by potential gradient, and convection driven by pressure gradient (Hwang 2010) – as shown in Equation (1):

$$J_i = -D\nabla c_i - \frac{Dz_i F c_i}{RT}\nabla \varnothing - vc_i \quad (1)$$

For ionic species i, J is the molar flux (mole·m^{-2}·s^{-1}), D is the diffusivity (m^2·s^{-1}), c is the molar concentration (mole·m^{-3}), z is the ionic charge, F is the Faraday constant (96,485 C·mole^{-1}), R is the universal gas constant (8.314 J·mole^{-1}·K^{-1}), T is the absolute temperature (K), $\varnothing$ is the electrical potential (volt), and v is superficial velocity (m·s^{-1}) (Mitko & Turek 2014).

The concentration gradient, which is the driving factor for the diffusion component of mass transport, is affected by several controllable factors, such as feed flow rate, feed concentration, feed pressure, applied voltage, and membrane characteristics. Although several studies have investigated the effects of these factors, previous studies have reported inconsistent effects for these factors such as feed flow rate, which significantly affects ion removal. Additionally, no study has yet investigated the effect of convection driven by pressure gradient on the concentration profile.

The inconsistent effects of feed flow rate have been reported in multiple published works. Aponte & Colón (2001) examined sodium chloride recovery from urine using the ED process, and they reported that at lower feed flow rates – which cause higher residence time – greater sodium chloride removal from urine was achieved (Aponte & Colón 2001). In contrast, Demircioglu *et al.* (2002) did not report any significant effect of feed flow rate on the removal of K^+ and Na^+ ions in their experiments (Demircioglu *et al.* 2002). Kabay *et al.* (2006) also did not observe any specific effect of feed flow rate on ion removal in their experiments (Kabay *et al.* 2006). In another inconsistent result, Sadrzadeh and Mohammadi reported both positive and negative effects of velocity on current efficiency in sea water treatment using a small ED system at different flow rates and different feed concentrations (Sadrzadeh & Mohammadi 2009).

The effects of feed concentration have also been investigated in previous works. Banasiak *et al.* (2007) investigated the effect of the initial sodium chloride concentration in the feed water, and their results confirmed that, at higher initial concentrations of sodium chloride in the feed solution, the rate of removal was greater (Banasiak *et al.* 2007). Despite the increase in removal percentage, Ali *et al.* (2010) showed that the total percent removal of ions decreased as the initial concentration of ions increased. Ali *et al.* qualified this result, however, explaining that salt removal was the same at the same hydrodynamic and electrical conditions, and stating that the reduction in percent removal was not observed but calculated from the equation for the percent removal of ions (Ali *et al.* 2010). Mohammadi *et al.* (2004) reported that increasing the initial feed concentration improved Pb_2^+ removal using ED in the range from 100 ppm to 500 ppm, but had no effect beyond 500 ppm (Mohammadi *et al.* 2004).

The effects of voltage have been investigated as well. It has been established that increasing voltage increases ion removal, and it has also been established that increased voltage affects some ions more than others. Walker (2010) showed that, at higher applied voltages, sodium and sulfate ions are removed faster relative to the total ion removal (Walker 2010). Kabay *et al.* (2006) also showed that voltage variation affects the removal of monovalent ions more than the removal of divalent ions under their experimental conditions (Kabay *et al.* 2006).

In 2000, Tanaka showed the current density distribution in an electrodialyzer is related to the distribution of flow velocity and electrolyte concentration in desalting cells theoretically and experimentally. The present study conducts laboratory research to provide additional information on how feed concentration, applied voltage, and feed flow rate affect salt removal and the concentration gradient in electrodialyzers. Additionally, the present study incorporates the effects of these factors into an experimental and mathematical model than can predict salt removal and concentration gradient. The present work builds on the efforts of Tanaka (2000), who modeled the concentration distribution in the direction of electric field (Tanaka 2000), as well as on other studies that developed a semi-empirical model based on Nernst–Planck and that tested the model for consistency against experimental data from various hydrodynamic conditions (Gnusin 2004; Gnusin *et al.* 2004). However, these studies have neglected the effect of convection driven by pressure gradient, which the present study takes into account.

MATHEMATICAL MODELING

A steady state fluid and mass transfer model was developed to simulate ion transport for NaCl in an ED cell pair. The model domain includes a two-dimensional cell pair where the electrical field is in the *y*-direction and water flows in the *x*-direction. Figure 1 shows more details of the computational domain, including the channel geometry and the associated coordinate system. The control volume is composed of an anion-exchange membrane (AEM), a cation-exchange membrane (CEM), and water channel. Table 1 presents the parameters and geometrical characteristics of the cell. The governing fluid and mass transfer equations are shown below.

Model equations

To couple the flow field and the mass transfer, a two-dimensional computational domain was created. Due to low flow velocity, a laminar flow regime was assumed for both fluid and mass transfer. Conservation of momentum and mass equations (Equations (2) through (5)) were used in Cartesian coordinates as follows:

$$\rho u_x \frac{\partial u_x}{\partial x} + \rho u_y \frac{\partial u_x}{\partial y} = \mu\left(\frac{\partial^2 u_x}{\partial x^2} + \frac{\partial^2 u_x}{\partial y^2}\right) - \frac{\partial P}{\partial x} - \rho \frac{\partial u_x}{\partial t}$$
$$\rho u_x \frac{\partial u_y}{\partial x} + \rho u_y \frac{\partial u_y}{\partial y} = \mu\left(\frac{\partial^2 u_y}{\partial x^2} + \frac{\partial^2 u_y}{\partial y^2}\right) - \frac{\partial P}{\partial y} - \rho \frac{\partial u_y}{\partial t} + f_y \quad (2)$$

$$u_x \frac{\partial c_i}{\partial x} + u_y \frac{\partial c_i}{\partial y} = D\left(\frac{\partial^2 c_i}{\partial x^2} + \frac{\partial^2 c_i}{\partial y^2}\right) - \frac{\partial c_i}{\partial t} \quad (3)$$

$$\frac{\partial u_x}{\partial x} + \frac{\partial u_y}{\partial y} = 0 \quad (4)$$

In Equation (2), the body force (f_y) is treated as follows:

$$f_y = \varepsilon E \frac{\partial^2 \varphi}{\partial y^2} \quad (5)$$

In this equation, ε ($C{\cdot}v^{-1}{\cdot}m^{-1}$) is electric permittivity, E ($v{\cdot}m^{-1}$) is the electric field, and φ is the electric potential.

Additional equations are used to develop the model (Dutta & Beskok 2001), which contains Equations (6) through (9). The Poisson–Boltzmann equation (Equation (6)) can be used to describe the electric potential distribution in the cell. In this equation, α is the ionic energy parameter and β is a variable. In Equation (8), ω is the Debye–Huckel parameter, which is the inverse of Debye length (λ). In Equation (9), e is the electron charge (C), k_b is the Boltzmann constant ($J{\cdot}K^{-1}$), and n_o is ion density ($mole{\cdot}m^{-3}$).

$$\frac{\partial^2 \varphi}{\partial y^2} = \beta\zeta \sinh\left(\alpha \frac{\varphi}{\zeta}\right) \quad (6)$$

$$\alpha = \frac{ez\zeta}{k_b T} \quad (7)$$

$$\beta = \frac{(\omega H)^2}{\alpha} \quad (8)$$

$$\omega = \frac{1}{\lambda} = \sqrt{\frac{8\pi n_0 e^2 z^2}{D k_b T}} \quad (9)$$

Numerically solving the incompressible Navier–Stokes equations is challenging for a variety of reasons. The first confounding factor is the nonlinear nature of the partial differential equations. Especially for flows of high velocity

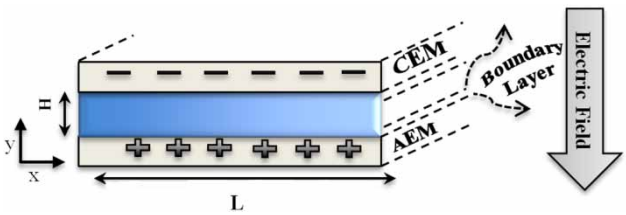

Figure 1 | Model geometry.

Table 1 | Parameters of the model

Parameter	Geometric characteristics	Description
D_{Na}	1.334e-9 [$m^2{\cdot}s^{-1}$]	Diffusion coefficient for Na^+
D_{Cl}	2.032e-9 [$m^2{\cdot}s^{-1}$]	Diffusion coefficient for Cl^-
D	80 [–]	Dielectric constant
d_a	0.6e-2 [m]	AEM thickness
d_c	0.6e-2 [m]	CEM thickness
H	0.4e-3 [m]	Channel width
L	0.08 [m]	Channel length
μ	8.98e-4 [Pa·s]	Water viscosity
ρ	1,000 [$kg{\cdot}m^{-3}$]	Water density
ζ	(−0.03 to 0.03) [v]	Zeta potential

or low viscosity, the equations can produce a highly unstable flow in eddy form. There is also the matter of the constraint imposed by incompressibility: any algorithm must ensure a divergence-free flow field at any given time during the calculation. This matter leads to the question of how to recover the pressure from the velocity, considering that the equations do not provide any boundary conditions for the pressure (Equation (10)) (Chapman 1967).

$$-\frac{1}{\rho}\left(\frac{\partial^2 p}{\partial x^2}+\frac{\partial^2 p}{\partial y^2}\right)=\left(\frac{\partial u_x}{\partial x}\right)^2+2\frac{\partial u_x}{\partial y}\frac{\partial u_y}{\partial x}+\left(\frac{\partial u_y}{\partial y}\right)^2 \quad (10)$$

Boundary conditions

The general fluid and mass boundary conditions are described below (Shaposhnik *et al.* 1997).

Fluid boundary conditions

At the inlets of the channels, the fluid velocity is uniform and specified:

$$u_x(0,y)=u_i, \quad u_y(0,y)=0$$

$$p(0,y)=p_{in}, \quad \frac{\partial p(L,y)}{\partial y}=0.$$

At the AEM and CEM, the no-slip boundary condition is applied for velocity. Consequently:

$$u_x(x,0)=u_y(x,H)=0$$

$$p(x,0)=p(x,H)=0.$$

Mass boundary conditions

At the inlets of the channels, the salt concentration is constant and specified:

$$c(0,y)=c_0=c_{Na+}=c_{Cl^-}$$

At the end of the channels, there is no diffusion flux, thus:

$$\frac{\partial c(L,y)}{\partial x}=0.$$

At the AEM, there is only anion flux, while at the CEM there is only cation flux. These conditions can be written as follows:

$$\frac{\partial c_{Na+}(x,0)}{\partial y}=\frac{i}{FD_{Na}}$$

$$\frac{\partial c_{Cl^-}(x,H)}{\partial y}=\frac{i}{FD_{Cl}}$$

Numerical procedure

The flowchart for the simulation of ED cell is shown in Figure 2. The simulation is based on an implicit finite difference method for each sub-model (fluid and mass transfer). As shown in Figure 2, at each time step, all internal iterations are performed until they converge, and then the simulation proceeds to the next time step.

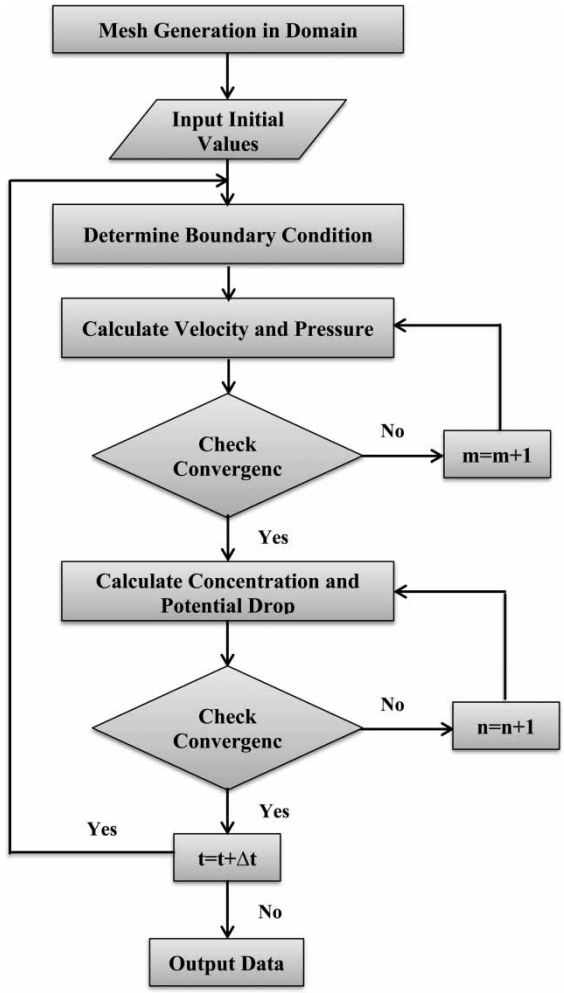

Figure 2 | Flowchart of the simulation process.

The model equations – including continuity, Navier–Stokes, and Nernst–Planck – were solved numerically, along with their appropriate bounding conditions, by using MATLAB software. The computational domain is discretized by a 160×30 grid. Detailed descriptions of the developed model were presented in Ghorbani *et al.* (2015).

EXPERIMENTAL METHODS

A complete laboratory-scale ED setup was designed and built to conduct the experiments where all the parameters were recorded every second using a data acquisition system. The system was run as a continuous system in which the effects of the investigated parameters could be detected clearly (Karimi 2015). Figure 3 shows the electrodialyzer for this experiment. Seven individual narrow tubes have been placed in between the channels to collect the sample at different time intercepts.

Cell and membrane

The ED cell unit used in this setup was PCCell ED 64 002, a laboratory-scale electrodialyzer made by PCCell GmbH Company with the nominal capacity of 4–8 L/h per dilute and concentrate cell.

The utilized CEMs and AEMs with the active area of 64 cm^2 were cut from GE CR67-HMR and GE AR908 membranes, respectively. The mesh spacer (Spacer-Gasket and End Spacer-Gasket) used in the stack to make the dilute and concentrate chambers had a thickness of 0.4 mm and a direct flow path.

ED setup

The setup consists of five tanks, three micro-gear pumps able to communicate with any personal computer and programmable logic controller, voltage transducers, a current transducer, a pressure transducer, and a flow meter. The operating conditions were monitored at the inlet and outlet of the stack using sensors for inline temperature, pH, conductivity, flow, and pressure. The schematic of the setup is shown in Figure 4.

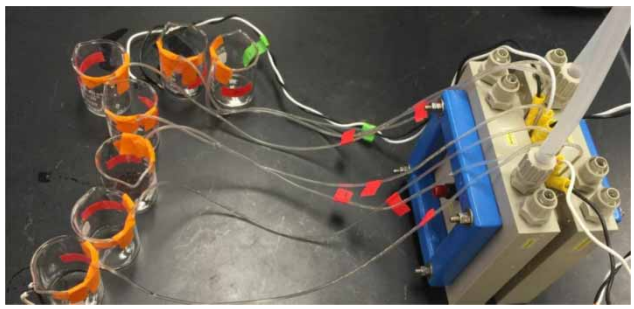

Figure 3 | PCCell ED 64 002 electrodialyzer.

Design of experiments

Based on the preliminary results, the final design of experiments was set as in Table 2. Experiments were conducted at a constant temperature (22 °C) and different feed concentrations, feed flow rates, feed pressures, and applied voltages (Table 3). The experiments were performed with a full factorial design at different levels of three main operating parameters. A full factorial design can determine the factors that significantly affect the response variables and can determine the optimum response in every set of the experiments (Montgomery 2008; Thompson 2011).

RESULTS AND DISCUSSION

Model validation

To assess the accuracy of the developed model, model validation was carried out by comparing the developed model with experimental values and Shaposhnik's model (Shaposhnik *et al.* 1997). The results are shown in Figures 5 and 6. For further model evaluation, the model's predicted concentration distribution along the dilute compartment was compared to the experimental values, as presented in Figure 6. The salt removal percentage was defined as:

$$\text{Salt removal} = \frac{C_f - C_p}{C_f} \times 100$$

where C_f is feed concentration and C_p is the concentration of the product.

As can be seen in Figure 5, the results of both models are close to each other and also match with experimental data. While Shaposhnik's model has a good agreement with experimental data, it cannot predict the concentration profile along the electrodialyzer. Figure 6 also illustrates the utility of the model developed in this research for predicting concentration distribution in dilute chamber along the electrodialyzer as a function of mono valent component concentrations. As can be seen in Figure 6, there is a good agreement between model and experimental results. And

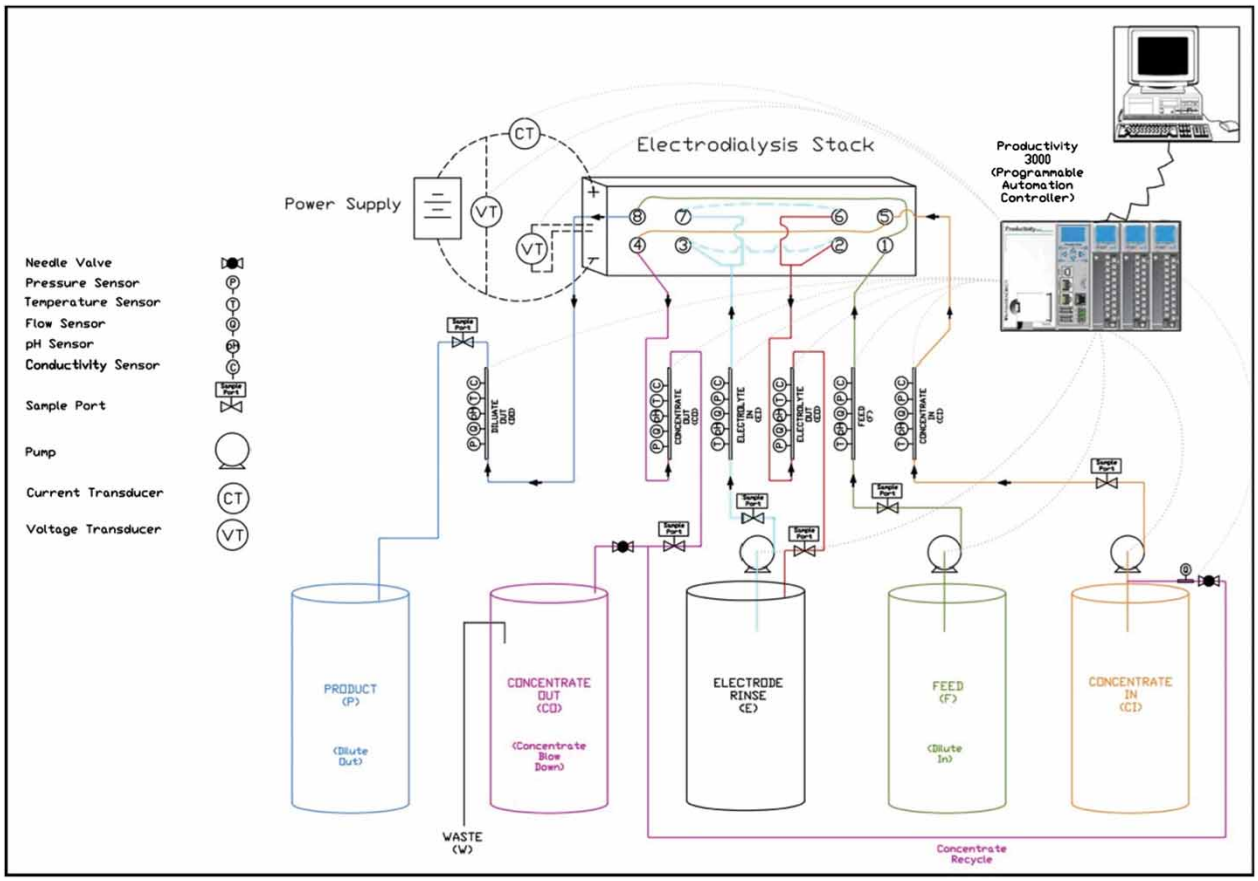

Figure 4 | Schematic of the setup.

Table 2 | Full factorial design of the experiments

Initial feed concentration level	Applied voltage level	Dilute in pressure level
1	1	1, 2, 3, 4, 5
	2	1, 2, 3, 4, 5
	3	1, 2, 3, 4, 5
	4	1, 2, 3, 4, 5
2	1	1, 2, 3, 4, 5
	2	1, 2, 3, 4, 5
	3	1, 2, 3, 4, 5
	4	1, 2, 3, 4, 5
3	1	1, 2, 3, 4, 5
	2	1, 2, 3, 4, 5
	3	1, 2, 3, 4, 5
	4	1, 2, 3, 4, 5
4	1	1, 2, 3, 4, 5
	2	1, 2, 3, 4, 5
	3	1, 2, 3, 4, 5
	4	1, 2, 3, 4, 5

Table 3 | Operating parameter levels of the experiments

Controllable factor	Factor level	Experimental value	
Feed concentration	1	600 ppm	
	2	1,000 ppm	
	3	1,500 ppm	
	4	2,000 ppm	
Voltage	1	7.0 Volt	
	2	8.0 Volt	
	3	10.0 Volt	
	4	12.0 Volt	
Pressure	1	1.00 Psi	(Re = 9)
	2	3.80 Psi	(Re = 16)
	3	5.00 Psi	(Re = 21)
	4	7.80 Psi	(Re = 30)
	5	12.0 Psi	(Re = 41)

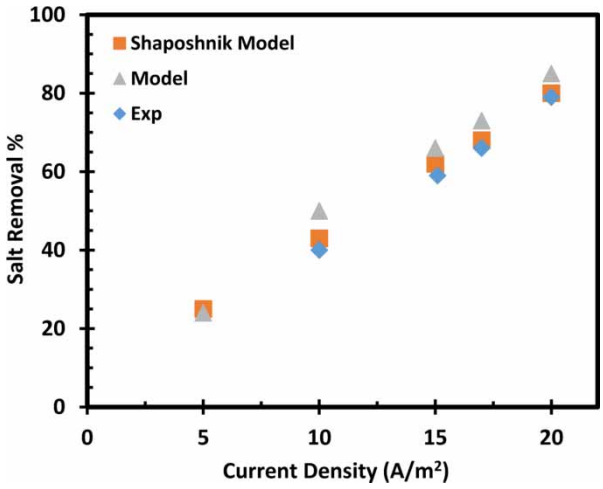

Figure 5 | Effect of current density on salt removal as shown by mathematical model and Shaposhnik model.

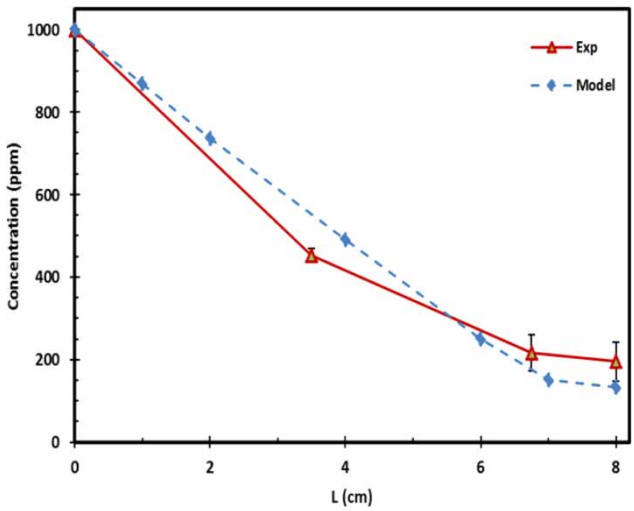

Figure 6 | Concentration distribution along the channel in the dilute compartment.

the maximum error is mostly in second half of the path where the most ion transport has already happened.

Concentration distribution along the channel

The concentration distributions along the dilute and concentrate compartments for four different feed concentrations are presented in Figure 7. The results show that the distribution is nonlinear, and as can be seen, most separation occurred in the first half of the path and as the fluid goes through the channel the separation become less. Because one of the factors that has effect on separation is ion concentration and, as the fluid passes through the channel, ion concentration reduces. The nonlinearity of distribution is mostly seen in

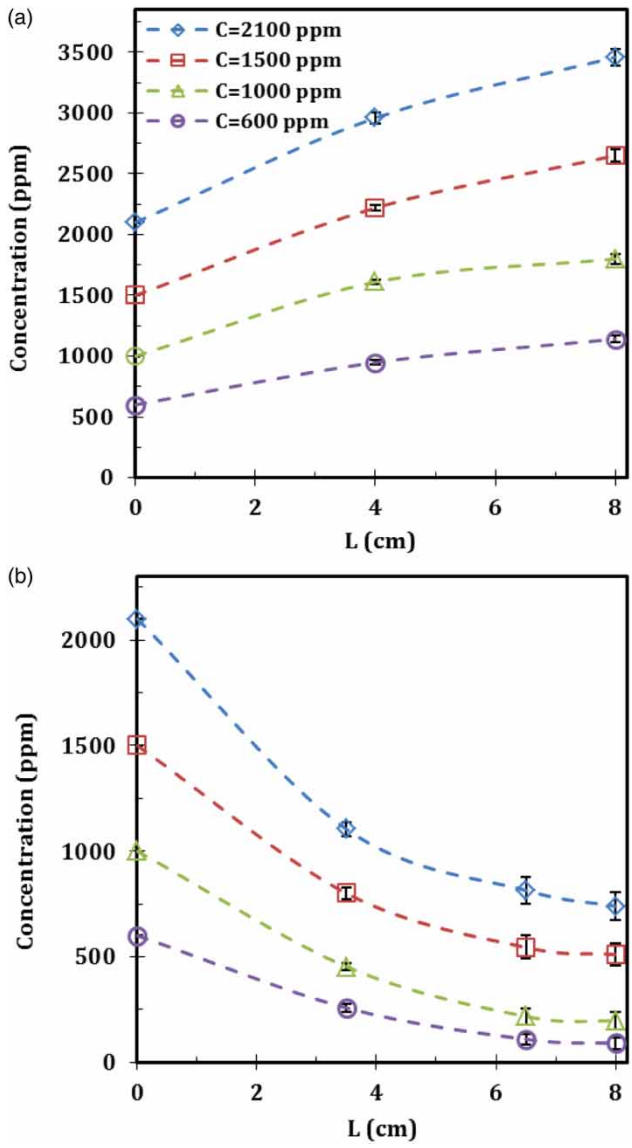

Figure 7 | Concentration distribution along the (a) concentrate compartment, (b) dilute compartment.

higher concentration. The rate of decrease was higher at high concentrations than at low concentrations.

Effect of different parameter on salt removal

Pressure

The negative effect of pressure on removal is shown in Figure 8, which presents the variation in salt removal with changes in current density at two different levels of pressure. At constant current density, salt removal decreased with increasing pressure.

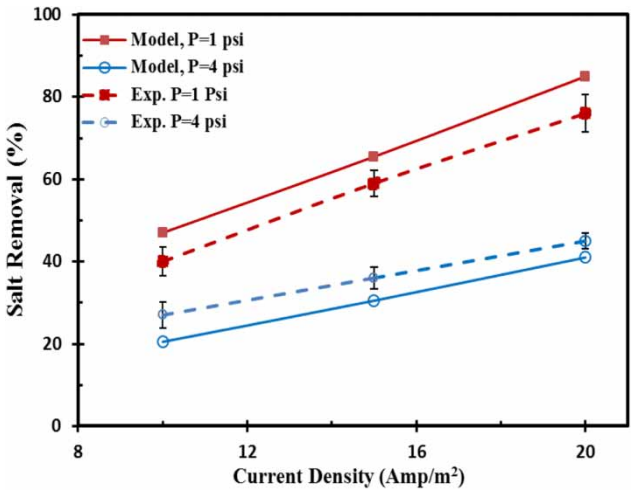

Figure 8 | Effect of current density on salt removal at different pressures.

Voltage

The most important factor that affects the rate of separation in the ED process is applied voltage. Applying greater voltage, which increases current density, increases the ion flux, which results in a decrease in ion concentration on the membrane surface (Moon *et al.* 2004) and a greater concentration gradient for each ion in the diffusion boundary layer (Dutta & Beskok 2001). The effect of cell voltage on salt removal at various feed concentrations and feed flow rates is shown in Figure 9. According to this figure, increasing cell voltage (particularly from 7 to 12 V) increases removal values at all flow rates and all feed concentrations. At lower flow rates, the proportion of increase in removal is higher than at higher flow rates, because a low flow rate means a low velocity, and at a low velocity there is

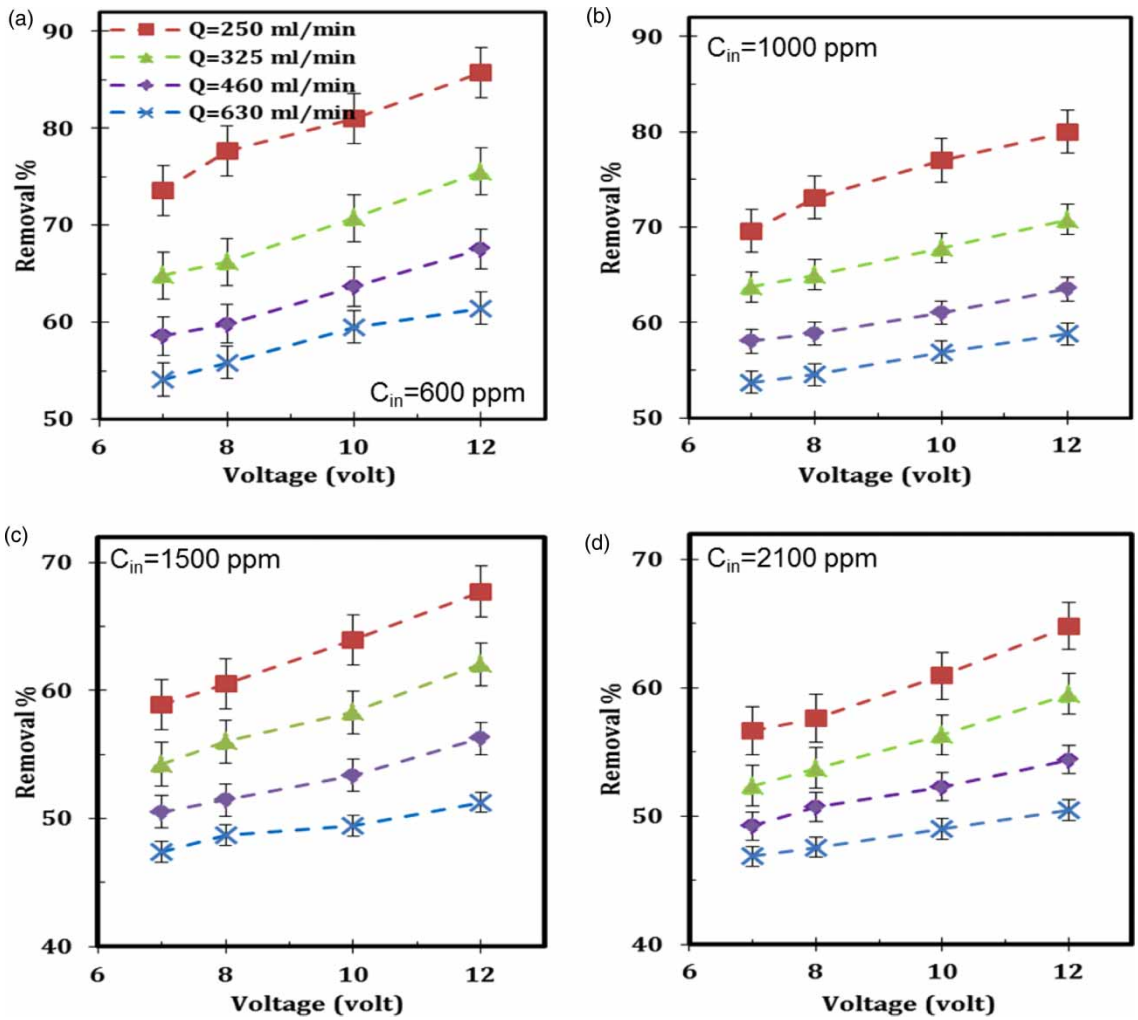

Figure 9 | Effect of voltage on salt removal at different flow rate: (a) $C_f = 600$ ppm, (b) $C_f = 1{,}000$ ppm, (c) $C_f = 1{,}500$ ppm, (d) $C_f = 2{,}100$ ppm.

enough time for ions to pass through the membrane. Higher concentration has lower removal percentage but, in fact, the amount of ions that has been removed is higher.

Flow rate

Flow rate (superficial velocity) can have either positive or negative effect on ion removal. Increased velocity may cause a positive effect on the rate of ion removal since increasing the velocity decreases the thickness of the diffusion boundary layer and increases the dilute concentration on the membrane surface according to following equations:

$$\delta_f = 4.91\sqrt{\frac{\mu x}{\rho u}} \tag{11}$$

$$Sc^{1/3} = \frac{\delta_f}{\delta_m} \tag{12}$$

where δ_f is fluid boundary layer and δ_m is mass boundary layer. However, increased flow rate may negatively affect the rate of ion removal because of lower residence time ($t_r = L/U$). In other words, it can be argued that at higher feed velocity, the ions do not have enough time to pass through the membrane or transfer from the dilute stream to the concentrate stream.

The effect of flow rate on salt removal at various levels of feed concentration and cell voltages is shown in Figure 10. According to these plots, increasing the feed flow rate, regardless of the feed concentration, will decrease the salt removal. As noted before, this effect is explained by reduced residence time at higher flow rates. Additionally, at higher flow rates

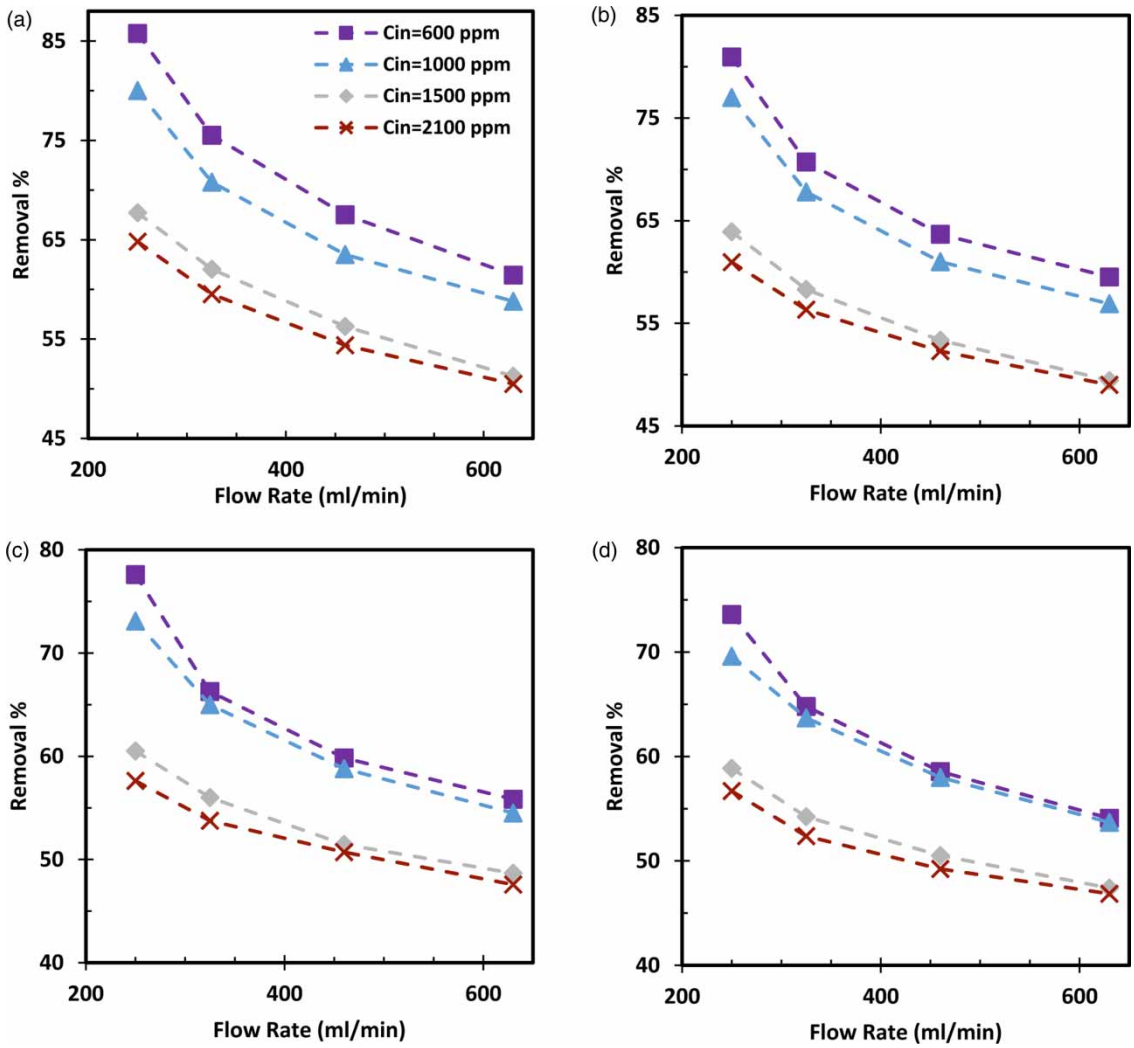

Figure 10 | Effect of flow rate on salt removal at different feed concentration: (a) V = 12 volts, (b) V = 10 volts, (c) V = 8 volts, (d) V = 7 volts.

and higher concentrations the effect of voltage is negligible. It means that at higher flow rate, applying higher voltage does not make any difference since ions do not have enough time.

Additionally, the effect of feed flow rate on removal is nonlinear, and the adverse effect of increases in the flow rate became more severe at higher flow rates. The nonlinear behavior can be explained by the hidden positive effect of superficial velocity on the thickness of the boundary layer, which affects ion removal.

CONCLUSIONS

A mathematical model was employed to predict mass transfer and the concentration distribution along the electrodialyzer. To further investigate the accuracy of the developed model, experimental results from a laboratory-scale ED system were compared to the model's predicted results for mass transfer and concentration distribution along the electrodialyzer. The findings of the experiment confirmed that the concentration distributions along both compartments are nonlinear and this nonlinearity is mostly seen at higher concentrations. The most separation occurred in the first half of the path. The equations used in the model were solved by the finite difference numerical method, using appropriate fluid and mass boundary conditions in the particular control volumes. Moreover, a predictive model was developed to predict the percentage of ion removal as a function of three driving forces.

Furthermore, the effects of different operating parameters (pressure, voltage, and flow rate) on the removal of ions were also investigated experimentally. The results show that higher pressure and higher feed flow rate (velocity) both had a negative effect on ion removal. By increasing the pressure or feed flow rate, the percent removal of ions decreased due to a reduction in the residence time.

The analysis of the results showed that the effect of feed flow rate on ion removal was nonlinear, a result that can be explained by the hidden positive effect of superficial velocity on the ion removal, which occurs because higher velocities reduce the thickness of the boundary layer. In the investigated ranges, increasing voltage resulted in increased salt removal at a specific feed concentration.

ACKNOWLEDGEMENTS

This work is supported by the Office of Naval Research (ONR). The authors also wish to thank Dr David Johnson to provide the schematic of the setup and his assistance in the experimental work.

REFERENCES

Ali, M. B. S., Mnif, A., Hamrouni, B. & Dhahbi, M. 2010 Electrodialytic desalination of Brackish Water: effect of process parameters and water characteristics. *Ionics* **16**, 621–629.

Aponte, V. M. & Colón, G. 2001 Sodium chloride removal from urine via a six compartment ED cell for use in advanced life support systems (Part 1: salt removal as a function of applied voltage and fluid velocity). *Desalination* **140**, 121–132.

Banasiak, L. J., Kruttschnitt, T. W. & Schäfer, A. I. 2007 Desalination using electrodialysis as a function of voltage and salt concentration. *Desalination* **205**, 38–46.

Chapman, T. W. 1967 *The Transport Properties of Concentrated Electrolytic Solutions*. PhD Thesis, University of California, Berkeley, CA, USA.

Demircioglu, M., Kabay, N., Kurucaovali, I. & Ersoz, E. 2002 Demineralization by electrodialysis – separation performance and cost comparison for monovalent salts. *Desalination* **153**, 329–333.

Dutta, P. & Beskok, A. 2001 Analytical solution of combined electroosmotic/pressure driven flows in two-dimensional straight channels: finite debye layer effects. *Analytical Chemistry* **73**, 1979–1986.

Ghorbani, A., Ghassemi, A., Andersen, P. & Foudazi, R. 2015 A prediction model of mass transfer through an electrodialysis cell. **57** (47), 22290–22303.

Gnusin, N. P. 2004 Modeling of mass electron transfer in an electrodialysis cell. *Theoretical Foundations of Chemical Engineering* **38** (3), 296–300.

Gnusin, N. P., Demina, O. A., Berezina, N. P. & Kononenko, N. A. 2004 Modeling of mass electro transfer in terms of the transport and structural properties of ion-exchange membranes. *Theoretical Foundations of Chemical Engineering* **38** (4), 394–398.

Hwang, S. 2010 Fundamentals of membrane transport. *Korean Journal of Chemistry Engineering* **28**, 1–15.

Kabay, N., Arda, M., Kurucaovali, I., Ersöz, E., Kahveci, H., Dal, S., Kopuzlu, S., Haner, M., Demircioğlu, M. & Yuksel, M. 2003 Effect of feed characteristics on the separation performance of monovalent and divalent salts by electrodialysis. *Desalination* **158**, 95–100.

Kabay, N., Kahveci, H., İpek, Ö. & Yüksel, M. 2006 Separation of monovalent and divalent ions from ternary mixtures by electrodialysis. *Desalination* **198**, 74–83.

Karimi, L. 2015 *Theoretical, Experimental and Predictive Modes for ion Removal in Electrodialysis Reversal*. PhD Thesis, New Mexico State University, Las Cruces, NM, USA.

Mitko, K. & Turek, M. 2014 Concentration distribution along the electrodialyzer. *Desalination* **341**, 94–100.

Mohammadi, T., Razmi, A. & Sadrzadeh, M. 2004 Effect of operating parameters on Pb_2^+ separation from wastewater using electrodialysis. *Desalination* **167**, 379–385.

Montgomery, D. C. 2008 *Design and Analysis of Experiments*, 7th edn. Wiley, Hoboken, NJ, USA.

Moon, P., Sandí, G., Stevens, D. & Kizilel, R. 2004 Computational modeling of ionic transport in continuous and batch electrodialysis. *Separation Science Technology* **39**, 2531–2555.

Sadrzadeh, M. & Mohammadi, T. 2009 Treatment of sea water using electrodialysis: current efficiency evaluation. *Desalination* **249**, 279–285.

Shaposhnik, V. A., Kuzminykh, V. A., Grigorchuk, O. V. & Vasileva, V. I. 1997 Analytical model of laminar flow electrodialysis with ion-exchange membranes. *Journal of Membrane Science* **133**, 27–37.

Strathmann, H. 2010 Electrodialysis, a mature technology with a multitude of new applications. *Desalination* **264**, 268–288.

Tanaka, Y. 2000 Current density distribution and limiting current density in ion-exchange membrane electrodialysis. *Journal of Membrane and Science* **173**, 179–190.

Thompson, J. R. 2011 *Empirical Model Building: Data, Models, and Reality*, 2nd edn. John Wiley and Sons, Inc., New Jersey.

Valerdi-Perez, R., Lopez-Rodriguez, M. & Ibáñez-Mengual, J. A. 2001 Characterizing an electrodialysis reversal pilot plant. *Desalination* **137**, 199–206.

Walker, W. S. 2010 *Improving Recovery in Reverse Osmosis Desalination of Inland Brackish Ground Waters via Electrodialysis*. PhD Thesis, The University of Texas at Austin, Austin, TX, USA.

Zhang, Y., Ghyselbrecht, K., Meesschaert, B., Pinoy, L. & Van der Bruggen, B. 2011 Electrodialysis on RO concentrate to improve water recovery in wastewater reclamation. *Journal of Membrane Science* **378**, 101–110.

First received 29 March 2017; accepted in revised form 13 October 2017. Available online 13 November 2017